 CMC, vol.32, no.1, pp.15-27, 2012

Prediction of Crack Location in Deep Drawing Processes Using Finite Element Simulation

S. K. Panthi[1] **and Sanjeev Saxena**[2]

Abstract: Sheet metal forming process like deep drawing subjected to large irreversible deformation. It leads to high strain localization zones and then internal or superficial micro defects. The deformation behavior and crack initiation in cylindrical deep drawing of aluminum alloy are simulated by the elasto-plastic finite element simulation. A1100-O and A2024-T4 sheet material are used in the simulation. Material properties based on the tensile and plane strain test is used in the simulation. Six cases are simulated in this study with different blank diameter. The simulated results are compared with the experimental results in terms of the crack location and critical punch displacement. The comparison of simulated results with experimental results shows a good agreement.

Keywords: Fracture, deep drawing process, finite element simulation

1 Introduction

Sheet metal forming processes are among the oldest and most widely used industrial manufacturing processes. These processes help in producing complicated shapes of thin walled parts of automotive panels and other structural parts. In such processes, an initial flat blank is plastically deformed in between the punch and the die. The blank is constrained on the periphery by a blank-holder. Among other sheet metal forming processes, deep drawing process is an important as it remarkably improve the productivity and the quality of the products. In deep-drawing process, the metallic material is subjected to large irreversible deformation, leading to high strain localization zones and then internal or superficial micro defects in the form of cracks due to the ductile damage (Khelifa et. al. 2007). Necking, crack formation and its growth cause quality problems which is an important ground for

[1] Corresponding Author: S. K. Panthi. Email: sanjay_panthi@yahoo.co.in; Tel.:+91 755 2457244; fax: +91 755 2488323; Postal Address: Computer Simulation & Process Modeling, CSIR-Advanced Materials and Process Research Institute (AMPRI), Bhopal (MP) India-462064

[2] CSIR-Advanced Materials and Process Research Institute (AMPRI), Bhopal (MP) India-462064

product refusal. These cracks formation are due to the ductile tearing of the sheet in the zones where it has attained its limit of plastic deformation. Therefore it is very important to predict the location of fracture initiation in deep drawing process and to find the process parameters that influence its location and crack formation. The finite element method in combination with fracture criteria seems to be the most promising aid for the prediction of cracks in sheet metal forming. In all fracture limit criteria, ductile fracture criterion has been proven to be an effective method to predict forming limit of various engineering materials, which is employed in sheet metal forming process.

The crack initiation in the deep drawing process has been carried out numerically and experimentally by many researchers in the past. For instance Ahmetoglu et al. (1995) studied the formability of rectangular part and determined the wrinkling and the fracture limits. Blank holder force control method is also developed to eliminate defects and to increase the drawing depth. Wan et al. (2001) analyzed the stress-strain states on the critical section of fracture in conical cup drawing and calculate the limit stress and limit load theoretically and verified it experimentally. Zhongqi et al. (2007) developed the ductile fracture criterion and evaluated the formability of the automotive aluminum sheet in deep drawing and stretching modes. By coupling elasto-plastic behavior and isotropic ductile damage in the 3D stamping operation Khelifa and Oudjene (2008) predicted that when and where the fracture can appear in the process. Ren et al. (2009) presented the warm deep drawing of magnesium alloy to predict the effects of the process parameters on the drawability of rectangular cups and the formation of the process defects. Micari et al. (1996) proposed an approach for the prediction of tearing in the deep drawing process of square boxes. The approach is based on a damage mechanics formulation. Takuda et al. (1999) carried out axisymmetric simulation of deep drawing to examine the application of ductile fracture criteria to predict the fracture initiation site and forming limit. Marumo et al. (1999) investigated the effect of the strain hardening characteristics and corner of die radii of square tools on the deep drawablity of square aluminum cups and concluded that these parameters highly influence the fracture in deep drawing process. Jain et al. (1998) developed a procedure for rapid determination of limiting drawing ratio (LDR), in deep drawing process of aluminum sheet materials, based on characteristic limit load. Berrahmoune et al. (2006) studied the delayed cracking phenomenon by determining the distribution of residual stresses and phase transformation after deep drawing of 301LN unstable austenitic steel. Yagami et al. (2007) investigated the effect of blank holder motion on wrinkle behavior in deep drawing process of Cu alloy by experimentally as well as numerically. Yoshihara et al. (2005) carried out the deep drawing process using magnesium alloy material and observed that the LDR can be improve by

applying the variable blank holder force (BHF) in comparison with constant BHF. Marumo and saiki (1998) introduced a characteristic force lines to determine the LDR and studied the effect of process parameters on deep drawablity of square cups. Hu et al. (2000) incorporated the void nucleation and growth model into a finite element code and studied the damage evolution in deep drawing process. Takuda et al. (1999) predicted the forming limit of magnesium based alloy AZ31 sheet by a combination of finite element and ductile fracture criterion and results were compared with experimental one. Mustafa et al. (1997) carried out the deep drawing of rectangular pan geometry of aluminum alloy to investigate the effect of blank shape and blank holder force on wrinkling and fracture. Gunnarsson et al. (1998) developed a blank holder system with degressive gas springs and evaluated it for axi-symmetric deep drawing process. Degressive, constant and progressive blank holder force trajectories were used to study the fracture and wrinkling in the process. Li et al. (2010) presented the experimental and numerical study of deep drawing process leading to intiation and propagation of cracks using the Mohr-Coloumb fracture criterion model. Liu et al. (2009) determined the material constant by the combination of FE simulation and tension tests and incorporated in ductile fracture criterion (DFC) model by yang and yu (2003) to predict the forming limit of aluminum alloy and steel sheets.

In the present study, 3D finite element simulation of deep drawing process was carried out to predict the location of crack initiation and know the parameters which affect its location. Two types of material were considered in the fracture analysis to find different geometrical parameters that influence the crack initiation in deep drawing process. The simulated results were compared with experimental results in terms of the location of the crack initiation. The numerically predicted variation in crack initiation location due to the change in blank diameter validate well with the experimental results.

2 Experimentation and material properties

In present study, finite element simulations were carried out using A1100-O and A2024-T4 sheet materials. The material properties used in the simulation are taken from literature (Takuda et. al. 1999). Table 1 shows the material properties used in the simulation. The tensile properties given in Table 1, are the average values of test results in 0^0, 45^0 and 90^0 to rolling direction.

The power law equation was used to define the material properties in the simulation. To predict the crack initiation in the deep drawing process fracture strain based properties was considered in the simulation. Table 2 shows the fracture strains in the tensile direction, ε_{1f}, derived from the measured reductions of area in uniaxial and plane-strain tension tests as reported in (Takuda et. al. 1999).

Table 1: Tensile properties used for the materials sheet

	A1100-O	**A2024-T4**
Strength coefficient (K) in power law (σ=K ε^n) (MPa)	179	749
Work-hardening exponent (n) in power law (σ=K ε^n)	0.26	0.19
Tensile strength (MPa)	96	479

Table 2: Fracture strains in tensile direction, ε_{1f} of materials in uniaxial and plane strain tension tests

	A1100-O	**A2024-T4**
ε_{1f} (uniaxial)	0.62	0.19
ε_{1f} (plane-strain)	0.42	0.14

3 Finite Element Simulation

To predict the location of crack initiation, static 3D finite element analyses of deep drawing process have been carried out using materials A1100-O and A2024-T4. The setup of the deep drawing process used in the analysis is shown in Fig. (1a). In the simulation punch, die and blank holder is considered as rigid body curved surfaces. The finite element models are analyzed under displacement control to simulate the experimental procedure. Large strain and large displacement relations based on geometry changes are assumed in the analysis. Six cases which are used in the simulation are given in Table 3. The diameter of the punch and the die are considered as 40 and 42.5 mm respectively for all the cases. It can be seen in Table 3 both the fracture strains obtained under uniaxial and plane strain test conditions are considered as separate case study.

Table 3: Geometric parameters used in the simulation

Case	Thickness of sheet	Tension test	Blank Diameter	Fracture Strain	Displacement	
					Exp.	FEM
I	1.0	Uniaxial	84 mm	0.62	14-15	13.4
II	1.0	Plane strain	80 mm	0.19	9-10	7.294
III	1.0	Plane strain	70 mm	0.19	–	12.91
IV	1.0	Uniaxial	84 mm	0.42	14-15	12.74
V	1.0	Plane strain	80 mm	0.14	9-10	5.623
VI	1.0	Plane strain	70 mm	0.14	–	11.03

FE analyses are performed with well-refined meshes in all cases. In the present analyses 8 noded linear hexahedral solid elements and linear wedge elements are used in the sheet model, with one element across the thickness direction. The simulation is also performed for two and three elements across the sheet thickness direction to see the effect of this on crack location. But it is found that it is not effect the location of crack initiation. A fine mesh is provided near the region of crack formation to predict accurately the variation of steep stress–strain. A typical mesh for the case-I is shown in Fig. (1b). The FE model has total 27202 nodes, 13400 linear hexahedral elements and 200 linear wedge elements. The displacement of the sheet was constrained by the contact boundary condition imposed by the rigid bodies. The punch is assigned an initial upward y-displacement where as constrained in x & z direction. For pursuing the analysis the stationary die and blankholder modeled as curved surfaces are constrained in all the directions. The simulation of deep drawing process is carried out in small number of incremental steps. As shown in Fig. (1a) the sheet rest on the blank holder and punch is moved upward gradually to deform the sheet. Once the contact is sensed between the punch and sheet the deformation is induced in the sheet and the sheet metal draws gradually. Fig. 2(a–d) describes the deformation shape for the deep drawing process corresponding to different stages of the punch displacement. This was numerically simulated by assigning the punch displacement and carried out up to the stage of crack formulation in the sheet.

4 Results & Discussion

The finite element simulation is carried out for the six cases as given in Table 3 to compare the results with experimental results in terms of crack location and punch displacement at which the crack formation take place in sheet. The experimentally observed fracture in the literature (Takuda et. al. 1999) due to necking around the punch corner in the deep drawing of A1100-O sheet having an initial blank diameter of 84 mm and thickness of sheet 1.0 mm is shown in Fig (3d). The simulation is also carried out under the same geometrical and process parameters to compare the location of fracture with the experimental one. The location of crack initiation by simulation is shown in Fig. 3 for case I. The von-mises, equivalent plastic strain and plastic dissipation energy density contours are also shown in Fig. 3. The critical punch displacement determined experimentally in between 14 and 15 mm while it is predicted as 13.4 mm by FE simulation. The results of simulation show a good comparison with experimental results in terms of the location of crack initiation. It is observed that the necking appears around the punch corner and that the deformation is localized there.

For case II the experimentally measured crack initiation in blank for A2024-T4

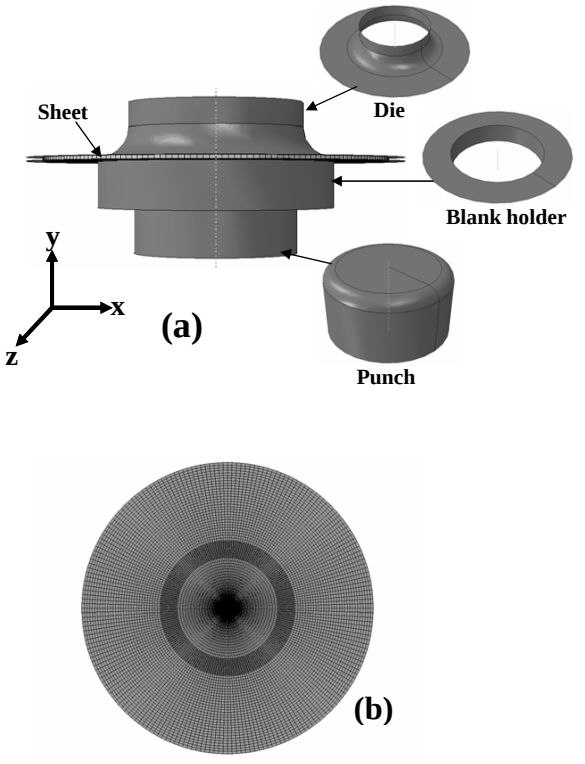

Figure 1: (a) Initial geometry of the deep drawing process (b) Initial blank with the finite element mesh for A1100-O material with diameter 84 mm diameterblank diameter

with an initial blank diameter 80 mm and thickness of sheet 1.0 mm is shown in Fig. (4d). The necking in blank is quite different from the necking as seen in A1100-O material blank. Crack initiation take place at the lower punch displacement or at early stage, as compared to A1100-O material, for this material at near the punch corner. The finite element simulations are performed under the similar condition to see the initial crack localization in the blank. It can be seen from Fig. 4 that crack initiate at the lower punch displacement as predicted by FE simulation also. The critical punch displacement for the case observed experimentally between 9 -10 mm while it is predicted as 7.3 mm by FE simulation. The von-mises, equivalent plastic strain and plastic dissipation energy density contours are also shown in Fig. 4 at predicted critical punch displacement (7.3 mm).

For case III, the experimental result for the 70 mm diameter blank is shown in Fig. (5d). It can be seen in experimental results that the fracture occurs in this case at

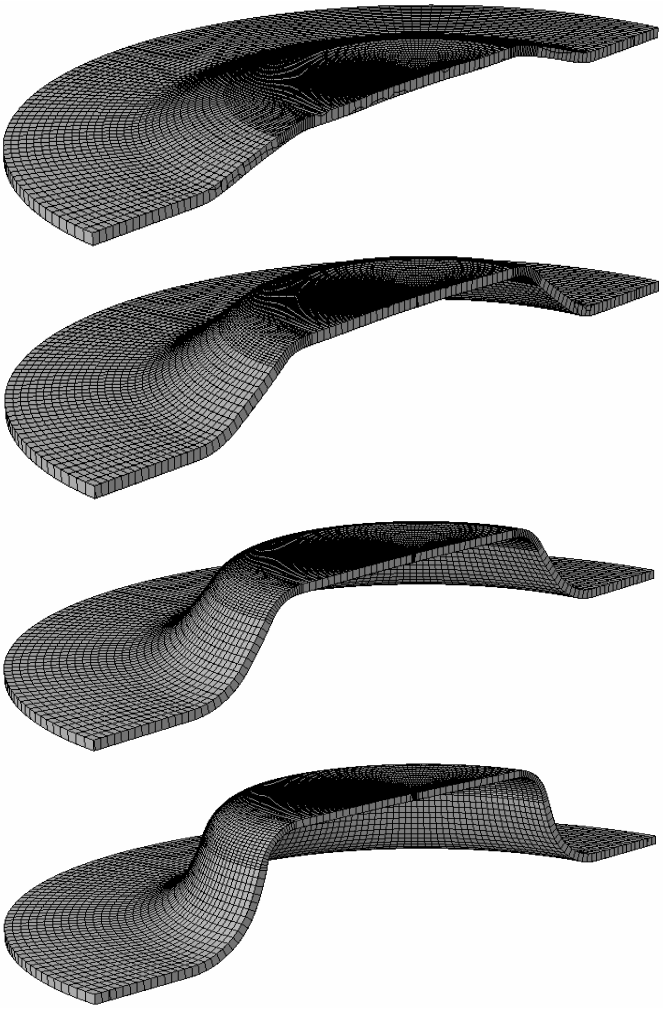

Figure 2: Deformed shape of the blank in deep drawing process (case I) at (a) 3.34 mm (b) 6.5 mm (c) 9.5 mm (d) 12.55 mm of punch displacement

the side wall of the drawn cup, apart from the previous two cases where fracture is observed near the punch corner. The simulation with A2024-T4 material and 70 mm blank diameter is also carried out to compare by experimental results in terms of location of crack initiation. The simulation was performed for the similar parameters. It is remarkable to see the difference in the fracture location for the same material have the different blank diameter. It is also observed that this necking

occurs at the large displacement of the punch as compared to 80 mm diameter blank. The difference in punch displacement means the difference in formality of sheet in both cases, with a lower diameter of blank high drawability can be achieved as compared to higher diameter of blank. The crack initiate in this case at the punch displacement of 12.91 mm as predicted in simulation. The von-Mises, equivalent plastic strain and plastic dissipation energy density contours are also shown in Fig. 5 at predicted critical punch displacement.

The finite element simulation is also carried out with the material properties obtained by the plane strain test. Simulation is performed for the geometric parameters for the case IV, V and VI as given in Table 3. It can be seen from Table 3, fracture occurred at the punch displacement of 12.74 mm and 5.263 mm for cases IV and V, respectively, which is lower than the punch displacement observed by simulation using the material properties determined by uni-axial tensile test. But it is observed that the location of fracture is same.

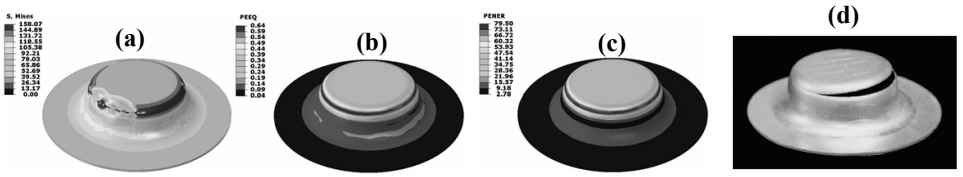

Figure 3: Comparison of experimental and FEM simulation results: Fracture around punch corner (A1100 sheet material, 84 mm blank diameter). (a) von-Mises stress (b) Equivalent plastic strain (c) Plastic dissipation energy density (d) Experimental results

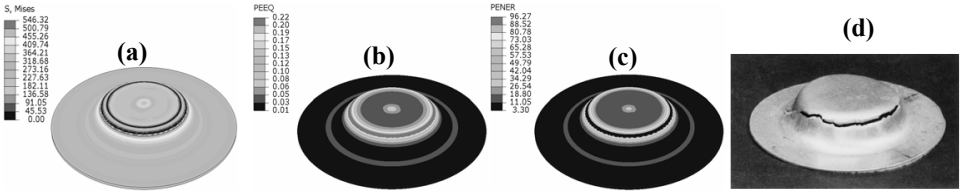

Figure 4: Comparison of experimental and FEM simulation results: Fracture around punch corner (A2024 sheet material, 80 mm blank diameter) (a) von-Mises stress (b) Equivalent plastic strain (c) Plastic dissipation energy density (d) Experimental results

The variation in thickness of sheet with punch displacement along the z-axis or in radial direction at different location i.e. from centre of the blank to the outer point

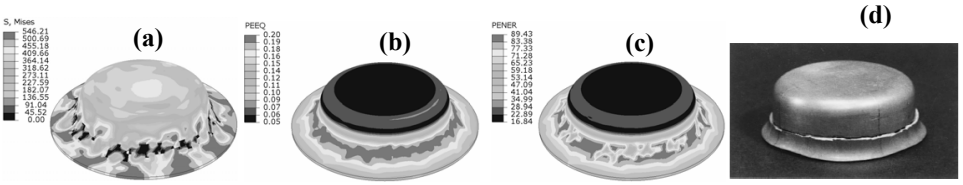

Figure 5: Comparison of experimental and FEM simulation results: Fracture around punch corner (A2024 sheet material, 70 mm blank diameter) (a) von-Mises stress (b) Equivalent plastic strain (c) Plastic dissipation energy density (d) Experimental results

of the blank is carried out by finite element simulation for the material A1100-O, A2024-T4. Fig. 6 shows the variation in sheet thickness with punch displacement for A1100-O material with the blank diameter of 84 mm (case I). The reduction in thickness of sheet is plotted between 5 mm to 42 mm from centre of sheet at the suitable increment. It can be seen from figure that the thickness remains constant or equivalent to initial thickness of sheet at the radial distance of 31.5, 35.25, 38.25 and 42 mm from the centre of the blank or in the outer region. Thickness decreases from the centre of the sheet and this reduction in thickness continue nearly upto 31.0 mm. The 20 % reduction in sheet thickness at the distance of 5, 10 and 19 mm can be seen from the plot. The maximum decrease in sheet thickness is observed in the region between 15 to 19 mm and maximum reduction at the distance of 17 mm from the centre which is approximately 40 % of initial thickness. Finally the crack initiation takes place in the region of between 15 to 19 mm. The start of initial crack initiation is observed at the punch displacement of 13.4 mm.

Two cases (II & III) are carried out for the material A2024-T4 with blank diameter of 80 & 70 mm. Fig. 7 shows the reduction in sheet thickness at different punch displacement for the blank diameter of 80 mm (case II). It can be seen from the plot that the thickness remains constant or equivalent to initial thickness of sheet i.e. 1 mm at the radial distance between 30 to 40 mm from the centre of the blank. The thickness remains nearly to 0.95 mm at the distance of 4.18, 8.15, 11.32, 13.71, 14.75, 15.25 mm from the centre. The thickness reduction reaches approximately 5 % at 15 mm from the centre. From 15 mm onward rate of reduction in thickness increases and the maximum thinning achieve in the region of 17 to 18 mm from the centre. The maximum reduction in thickness reaches by 20 % of initial sheet thickness approximately. The reduction in thickness beyond 18 mm is less and it reaches approximately 5 % at the distance of 30 mm from the centre. In this case the reduction in thickness is less as compared to A1100-O material case. Therefore, it is observed that the localized necking occurs at the early stage in A2024-T4

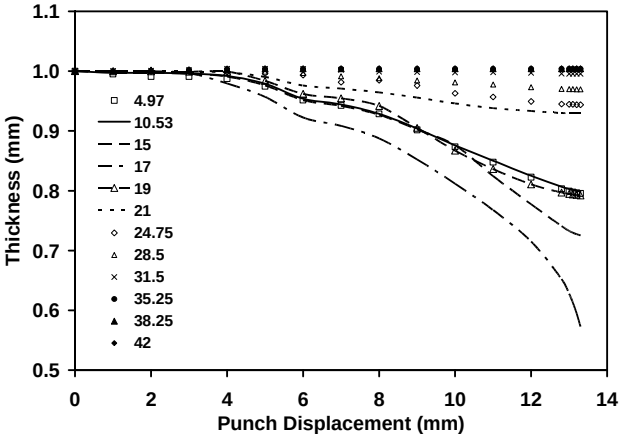

Figure 6: Variation in sheet thickness in radial direction with punch displacement for A1100-O material sheet with blank diameter 84mm.

material sheet with 80 mm blank diameter as compare to A1100-O material with 84 mm blank diameter. The crack initiate at the punch displacement of 7.3 mm experimentally, while it is predicted 9.0 mm by Finite element simulation.

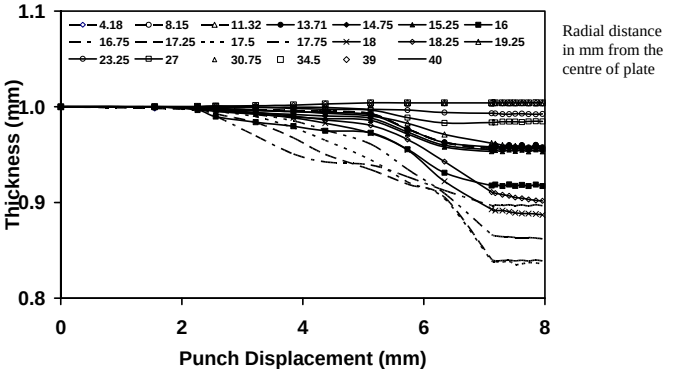

Figure 7: Variation in sheet thickness in radial direction with punch displacement for A2024 material sheet with blank diameter 80 mm.

The reduction in thickness of sheet with punch displacement for A2024-T4 material sheet with 70 mm blank diameter (case III) is shown in Fig. 8. It can be seen from graph that the maximum reduction in thickness of the sheet is only 6 % upto the 12 mm punch displacement. The uniformity in thickness of sheet is higher in this case as compare to previous two cases. Maximum reduction in thickness of sheet is

observed at nearly 17.75 mm upto 12 mm punch displacement. As the punch move further to deform the sheet a crack initiation is observed suddenly at the distance 26.88 mm from the centre, which finally converted in the fracture. The predicted pattern of location of crack initiation is approximately close to the experimental one. In this case the reduction in thickness is observed between 5 to 7 % for most of the region. The thickness remains nearly same to the initial sheet thickness from 27 to 35 mm.

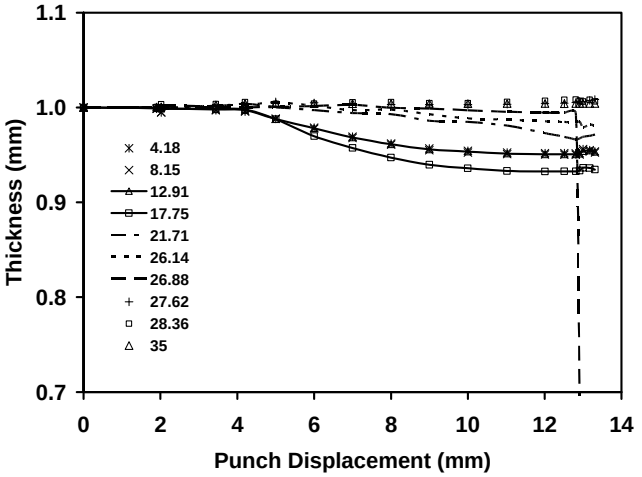

Figure 8: Variation in sheet thickness in radial direction with punch displacement for A2024 material sheet with blank diameter 70 mm.

5 Conclusions

In the present study, 3D numerical simulation has been carried out for six cases considering A1100-O and A2024-T4 materials to predict the location of crack in deep drawing process. The diameter of blank was used 84 mm with A1100-O material while 80 mm and 70 mm diameter blank was used with A2024-T4 material. The effect of blank diameter on location of crack initiation has been carried for A2024-T4 material. Fracture strain was used in the simulation based on the uniaxial and plane strain tensile test. Three cases were considered to compare the simulation results with experimental results in terms of location of crack. The following conclusions emerge from this study:

- In the present study it is found through numerical study that the location of crack formation depends on the blank diameter which resembles well with

the experimental observations.

- In deep drawing process of sheet, the numerical prediction of crack formation is better predicted by using fracture strain value obtained in uni-axial tensile test as compared to fracture strain value obtained in plane strain specimen test.

- The reduction in sheet thickness is found to depend on blank diameter. It can also be concluded that blank diameter in deep drawing process affects the drawability or formability of sheet.

References

Ahmetoglu, M., Broek, T.R., Kinzel, G., et al., (1995): Control of blank holder force to eliminate wrinkling and frature in deep-drawing rectangular parts. *Annals of the CIRP* 44 (1), 247-250.

Berrahmoune, M.R., Berveiller, S., Inal, K., et al., (2006): Delayed cracking in 301LN austenitic steel after deep drawing Martensitic transformation and residual stress analysis. *Materials Science and Engineering A* 438–440, 262–266.

Gunnarsson, L., Asna?, N., Schedin, E., (1998): In-process control of blank holder force in axi-symmetric deep drawing with degressive gas springs. *Journal of Materials Processing Technology* 73, 89–96.

Hu, J.G., Ishikawa, T., Jonas, J.J., (2000): Finite element analysis of damage evolution and the prediction of the limiting draw ratio in textured aluminum sheets. *Journal of Materials Processing Technology* 103, 374-382.

Jain, M., Allin, J., Bull, M.J., (1998): Deep drawing characteristics of automotive aluminum alloys. *Materials Science and Engineering A* 256, 69–82.

Khelifa, M., Oudjene, M., Khennane, A., (2007): Fracture in sheet metal forming: Effect of Ductile damage evolution. *Computers and Structures* 85, 205-212.

Khelifa, M., Oudjene, M., (2008): Numerical damage prediction in deep-drawing of sheet metals. *Journal of Materials Processing Technology* 200, 71–76.

Liu, H., Yang, Y., Yu, Z., et al., (2009): The application of a ductile fracture criterion to the prediction of the forming limit of sheet metals. *Journal of Materials Processing Technology* 209, 5443–5447.

Li, Y., Luo, M., Gerlach, J., et al., (2010): Prediction of shear-induced fracture in sheet metal forming. *Journal of Materials Processing Technology* 210, 1858–1869.

Marumo, Y., Saiki, H., (1998): Evaluation of the forming limit of aluminum square cups. *Journal of Materials Processing Technology* 80–81, 427–432.

Marumo, Y., Saiki, H., Mori, T., (1999): Combined effects of strain hardening characteristics and tool geometry on the deep-drawability of square aluminum cups. *Journal of Materials Processing Technology* 89-90, 30–36.

Micari, F., Fratini, L., Casto, S., et al., (1996): Prediction of ductile fractures occurrence in deep drawing of square boxes. *Annals of the CIRP* 45(1), 259-262.

Mustafa, A., Ahmetoglu, G. K., Altan, T., (1997): Forming of aluminum alloys—application of computer simulations and blank holding force control. *Journal of Materials Processing Technology* 71, 147-151.

Ren, L.M., Zhang, S.H., Palumbo, G., et al., (2009): Numerical simulation on warm deep drawing of magnesium alloy AZ31 sheets. *Materials Science and Engineering A* 499, 40–44.

Takuda, H., Mori, K., Hatta, N., (1999): The application of some criteria for ductile fracture to the prediction of the forming limit of sheet metals. *Journal of Materials Processing Technology* 95, 116-121.

Takuda, H., Yoshii, T., Hatta, N., (1999): Finite-element analysis of the formability of a magnesium-based alloy AZ31 sheet. *Journal of Materials Processing Technology* 89–90, 135–140.

Wan, M., Yang, Y., Li, S., (2001): Determination of fracture criteria during the deep drawing of conical cups. *Journal of Materials Processing Technology* 114, 109-113.

Yagami, T., Manabe, K., Yamauchi, Y., (2007): Effect of alternating blank holder motion of drawing and wrinkle elimination on deep-drawability. *Journal of Materials Processing Technology* 187–188, 187–191.

Yang, Y., Yu, Z., Li, X., et al., (2003): A new ductile fracture criterion and its application to the prediction of forming limit in deep drawing. *Journal of Materials Science and Technology* 19, 217–219.

Yoshihara, S., Manabe, K., Nishimura, H., (2005): Effect of blank holder force control in deep-drawing process of magnesium alloy sheet. *Journal of Materials Processing Technology* 170, 579–585.

Yu, Z., Lin, Z., Zhao, Y., (2007): Evaluation of fracture limit in automotive aluminum alloy sheet forming. *Materials and Design* 28, 203–207.